

# Novel Adaptive Generalized Likelihood Ratio Detector with Application to Maneuvering Target Tracking

Dany Dionne\* and Hannah Michalska†  
McGill University, Montreal, Quebec H3A 2A7, Canada

and

Yaakov Oshman‡ and Josef Shinar§  
Technion—Israel Institute of Technology, 32000 Haifa, Israel

**A novel adaptive jump-detection algorithm is introduced for scenarios involving abrupt changes in the inputs to linear systems, such as those that might occur in tracking maneuvering targets. Improving upon the standard generalized likelihood ratio (GLR) detector, presented over two decades ago, the new algorithm is characterized by increased robustness with respect to uncertainties in the system input, which frequently arise in the context of target tracking applications. The performance of the new algorithm is demonstrated in an endgame scenario involving an interceptor missile and a maneuverable tactical ballistic missile. An extensive Monte Carlo simulation study is used to demonstrate the superiority of the method over the conventional GLR method in terms of its much smaller observed false alarm probability, which actually agrees with the theoretical value. The new algorithm also facilitates a correct isolation of the abrupt change, is consistent in the usual statistical sense, and generally proves more reliable.**

## I. Introduction

**M**ANY stochastic processes encountered in applications such as maneuvering target tracking, pattern recognition, and fault detection are characterized by the occurrence of abrupt changes at unknown time instants. An abrupt change is defined as a rapid change (a change that occurs over a single sampling interval) in the probability density function of the process (see Ref. 1, p. 1). Such abrupt changes are usually diagnosed by employing specialized detector algorithms.<sup>2</sup> This diagnosis task is performed in a two-stage manner (see Ref. 3, p. 218) in the first stage (referred to as detection), a decision is made whether an abrupt change has indeed occurred; in the second stage (referred to as isolation), the abrupt change is confirmed, and its estimated parametric characteristics are accepted as valid.

There is an inherent delay between the moment at which an abrupt change occurs and the time instant at which it is detected. This detection delay stems from the need to collect sufficient information to render a detection with some reliability (usually, with respect to a prespecified false alarm probability). The minimum average delay of detection is achieved by Bayesian detectors.<sup>4</sup> Unfortunately, optimal Bayesian detectors are in general not finite dimensional whenever the value of the system input after the change is unknown, as it is frequently encountered in target tracking applications (see Ref. 5, p. 23). A finite dimensional alternative in such systems is provided by the class of generalized likelihood ratio (GLR) type detectors. GLR-type detectors have been shown to be asymptotically optimal under several criteria related to quickest detection.<sup>6</sup> In previous studies,<sup>7,8</sup> the “standard” GLR detector algorithm<sup>9</sup> has been applied

successfully to maneuver detection. These studies assumed the target maneuver to be unknown; however, the system inputs before the maneuver were assumed known. As demonstrated in this paper, in situations in which the values of the system inputs are unknown both before and during the target maneuver, the standard GLR detector algorithm<sup>9</sup> exhibits a degraded false alarm probability and often fails to isolate the change correctly.

A new detection algorithm, termed adaptive- $\mathcal{H}_0$  GLR detector, is introduced herein to alleviate the aforementioned phenomenon whenever the inputs are unknown both before and during the maneuver. The new method can be viewed as a generalization of the GLR detector to isolate additive abrupt changes in unknown inputs to linear systems. As the standard GLR detector does, the adaptive- $\mathcal{H}_0$  GLR detector assumes a realization for the unknown inputs before the abrupt change; the latter is referred to as the “reference realization.” However, in contrast with the standard GLR algorithm, the reference realization now belongs to a parametric family of functions whose parameter is estimated online. Hence, the new algorithm is equipped with the ability to adapt, online, its reference realization conditioned on the measurements received, thus alleviating the need for an a priori and exact realization of the unknown inputs before the abrupt change.

In applications involving a maneuvering target, the ability to quickly and reliably diagnose target maneuvers permits the improvement of state estimation<sup>10</sup> and guidance.<sup>11</sup> In an example application to an endgame scenario involving the interception of a maneuvering tactical ballistic missile (TBM), the adaptive- $\mathcal{H}_0$  algorithm proves to be more robust with respect to uncertainties in the target maneuvers than the standard GLR detector. Specifically, it is shown to provide a false alarm probability, which is four times smaller than that of the standard GLR detector. Additionally, and contrary to the standard GLR detector, this false alarm probability matches the corresponding theoretical probability calculated as a function of the threshold parameter of the GLR test. The new algorithm is also shown to be more reliable in the isolation of the target maneuvers.

The remainder of this paper is organized as follows. The problem statement is formulated in the next section. A general description of the GLR detection procedure is then presented, followed by an outline of the standard GLR detector algorithm.<sup>9</sup> The main contribution of this paper, which is the adaptive- $\mathcal{H}_0$  GLR detection algorithm, is presented next. In the next section, the adaptive- $\mathcal{H}_0$  detector is implemented and tested in a missile guidance endgame scenario, involving the interception of a randomly maneuvering TBM. This

Received 20 September 2004; revision received 24 March 2005; accepted for publication 1 May 2005. Copyright © 2006 by the authors. Published by the American Institute of Aeronautics and Astronautics, Inc., with permission. Copies of this paper may be made for personal or internal use, on condition that the copier pay the \$10.00 per-copy fee to the Copyright Clearance Center, Inc., 222 Rosewood Drive, Danvers, MA 01923; include the code 0731-5090/06 \$10.00 in correspondence with the CCC.

\*Graduate Student, Centre for Intelligent Machines, 3480 University Street. Student Member AIAA.

†Professor, Centre for Intelligent Machines, 3480 University Street.

‡Associate Professor, Department of Aerospace Engineering. Associate Fellow AIAA.

§Professor Emeritus, Department of Aerospace Engineering. Fellow AIAA.

scenario is used to assess and demonstrate the detection and isolation capabilities of the new detector via an extensive Monte Carlo simulation, in which the new adaptive- $\mathcal{H}_0$  and the standard GLR detectors are compared. Concluding remarks are provided in the final section.

## II. Problem Statement

For simplicity, discrete-time stochastic linear systems are considered whose models take the following form:

$$x(k+1) = F(k)x(k) + G_1(k)u(k) + G_2(k)z(k) + \epsilon(k)$$

$$x \in \mathbb{R}^n, u \in \mathbb{R}^r, z \in \mathbb{R}^s \quad (1)$$

$$y_m(k) = H(k)x(k) + \eta(k), \quad y_m \in \mathbb{R}^p \quad (2)$$

where  $\epsilon(k) \sim \mathcal{N}[0, Q_\epsilon(k)]$  and  $\eta(k) \sim \mathcal{N}[0, Q_\eta(k)]$ . It is assumed that  $u$  is a known input function,  $z$  is an unknown input function subject to additive abrupt changes,  $y_m$  is a measurement, and  $w$  and  $\eta$  are independent Gaussian sequences representing the process and measurement noises, respectively. It is further assumed that the inputs  $u$  and  $z$  are bounded, so that

$$|u(k)| \leq u^{\max}, \quad |z(k)| \leq z^{\max}, \quad \text{a.e.} \quad k = 0, 1, \dots \quad (3)$$

Let  $k^*$  denote the time instant of the most recent abrupt change. For practical reasons, it is assumed that the length of the time interval between successive abrupt changes is bounded from below by  $w^*$ .

The problem is to diagnose, online, abrupt changes in the system (1) and (2). The diagnosis task requires minimizing the average detection delay, the false alarm probability, and the error in the estimated value of  $z$ .

## III. Standard GLR Detector

In the context of the problem specified, the task of the detector is to provide a full diagnosis of the unknown input  $z$ . First presented in Ref. 9, the idea behind the standard GLR detection algorithm is to test a number of prespecified hypotheses concerning the past history of  $z$ . The GLR test employs ratios of likelihood functions matched to these hypotheses. The test belongs to the class of sequential probability ratio test algorithms. The detection algorithm calculates the likelihood ratios using the time series of residuals (innovations process) generated by a single Kalman filter. This Kalman filter is designed to act as a whitening filter over time intervals with no abrupt changes. The GLR detector also yields a maximum likelihood (ML) estimate of the onset time of the abrupt change and a ML estimate of the realization of the unknown input after the change:  $z(l)$ ,  $l \in [k^*, k]$ .

At any time instant  $k$ , the input signals to the GLR detection procedure are 1) the measurements  $y_m(k)$ , and 2) the set of hypotheses  $\mathcal{S}^k$  (defined in Sec. III.A) for  $k \geq 0$ . Let  $\mathcal{E}(k)$  be a binary indicator random variable (the detection indicator), such that

$$\mathcal{E}(k) \triangleq \begin{cases} 1 & \text{An abrupt change has been detected at time } k \\ 0 & \text{otherwise} \end{cases} \quad (4)$$

Similarly, let  $\mathcal{E}^R(k)$  be a binary indicator random variable (the isolation indicator), such that

$$\mathcal{E}^R(k) \triangleq \begin{cases} 1 & \text{An abrupt change has been detected at time } k \\ 0 & \text{otherwise} \end{cases} \quad (5)$$

The output signals from the GLR detection procedure are 1) the estimated onset time of the abrupt change  $\hat{k}^*$ , 2) the estimated value  $\hat{z}_{\text{ML}}$  of the unknown input  $z$  after the change (this also necessitates identifying the class of parametric functions to which  $z$  belongs), 3) the state of the detection indicator  $\mathcal{E}(k)$ , and 4) the state of the isolation indicator  $\mathcal{E}^R(k)$ . Figure 1 depicts a schematic block diagram of the standard GLR algorithm.

The state of the pair  $\{\mathcal{E}(k), \mathcal{E}^R(k)\}$  describes one of the following mutually exclusive situations:

1)  $\{\mathcal{E}(k), \mathcal{E}^R(k)\} = \{0, 0\}$ : in this case no abrupt change has been detected at  $t = k$ . All past detected abrupt changes, if any, have been isolated.

2)  $\{\mathcal{E}(k), \mathcal{E}^R(k)\} = \{1, 0\}$ : in this case an abrupt change has been detected at time  $k$ , which has not yet been isolated.

3)  $\{\mathcal{E}(k), \mathcal{E}^R(k)\} = \{1, 1\}$ : in this case an abrupt change has been detected and isolated at time  $k$ . To allow for the detection of subsequent abrupt changes, the states of both indicators are reset to zero at time instant  $k+1$ , that is,  $\{\mathcal{E}(k+1), \mathcal{E}^R(k+1)\} = \{0, 0\}$  (unless another abrupt change has been detected at time  $k+1$ , in which case  $\{\mathcal{E}(k+1), \mathcal{E}^R(k+1)\} = \{1, 0\}$ ).

Using the detection and isolation indicators, a false detection (false alarm) event is defined as the event that results in the sequence  $\{\mathcal{E}(k-1) = 1, \mathcal{E}^R(k-1) = 0, \mathcal{E}(k) = 0, \mathcal{E}^R(k) = 0\}$ . The various cases described herein are shown schematically in Fig. 2. The procedures for determining the values of the binary variables  $\mathcal{E}$ ,  $\mathcal{E}^R$  are outlined in the sequel.

The GLR algorithm is sequential in nature, as concisely detailed in the ensuing, and its computational load increases linearly with the number of considered hypotheses. For a more complete description, the interested reader is referred to Ref. 9.

### A. Set of Hypotheses

A finite set of hypotheses  $\mathcal{S}^k = \{\mathcal{H}_0, \mathcal{H}_1, \dots, \mathcal{H}_N\}$  is first introduced to adequately describe all relevant realizations of the time

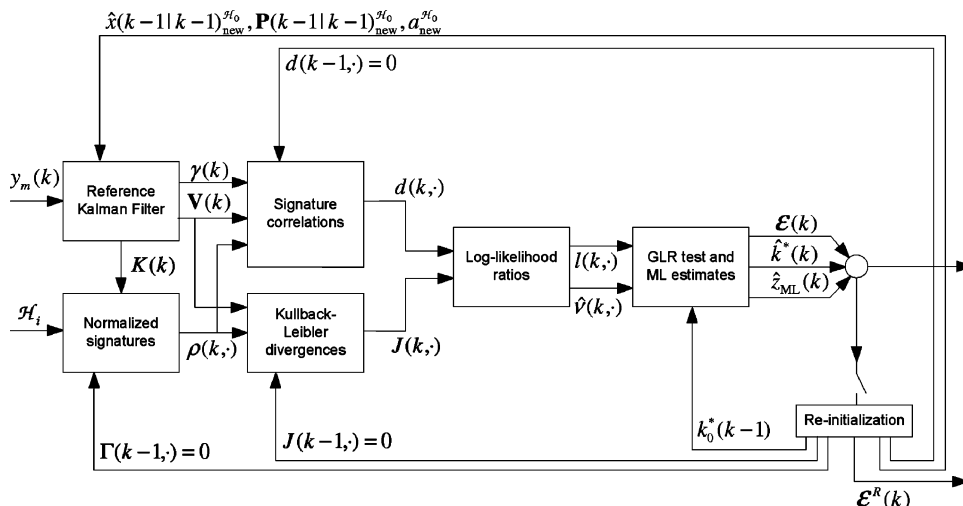


Fig. 1 Schematic flow diagram of the standard GLR detector.

$\mathcal{E}$	0	0	0	0	0	0	1	1	1	0	0	0
$\mathcal{E}^R$	0	0	0	0	0	0	0	0	1	0	0	0
Event	J			D			I&R					

Time  $\rightarrow$

**a) Detection and isolation of a single abrupt change**

$\mathcal{E}$	0	0	0	0	0	0	1	0	0	0	0	0
$\mathcal{E}^R$	0	0	0	0	0	0	0	0	0	0	0	0
Event							D					

Time  $\rightarrow$

**b) False detection**

$\mathcal{E}$	0	0	0	0	1	1	1	1	1	0	0	0
$\mathcal{E}^R$	0	0	0	0	0	0	1	0	1	0	0	0
Event 1	J		D		I&R							
Event 2	J			D			I&R					

Time  $\rightarrow$

**c) Detection and isolation of two close-by abrupt changes**

**Fig. 2** Detection and isolation indicators' states: **J**, jump; **D**, detection; **I&R**, isolation and reset of both indicators.

series  $z$ . This set of hypotheses must be updated at each current time instant  $k$ . Each hypothesis  $\mathcal{H}_i \in \mathcal{S}^k$  corresponds to an assumption about the *absolute* onset time of the abrupt change  $k_i^*(k)$  and an assumption about the possible class of parametric functions that adequately characterizes the shape of the change. The hypotheses describe at most a single hypothetical abrupt change. Hence, the hypotheses describe the realization of the time series  $z$  only in the time interval  $[k_0^*, k]$ , where  $k_0^*$  is the absolute onset time instant of the last known change in  $z$ .

Let  $\{f_i(\cdot, k_i^*)\}_{i=1}^N$  be a set of basis functions, representing all feasible classes of abrupt change functions at time  $k$ . A particular shape of a change will then be referred to as  $f_i(l, k_i^*)$ , for some  $i \in \{1, 2, \dots, N\}$ , whereas the actual change function would be  $v_i f_i(l, k_i^*)$ ,  $l \in [k_i^*, k]$ , where  $v_i$  is the change intensity. The GLR hypotheses do not require an assumption about the actual value of the change intensity, as this value will be estimated later on by scaling. The members of the set of hypotheses  $\mathcal{S}^k$  are, hence, defined as follows:

$$\mathcal{H}_0 : z(l) = a^{\mathcal{H}_0}(l), \quad l = k_0^*, \dots, k \quad (6a)$$

$$\mathcal{H}_i : z(l) = a^{\mathcal{H}_0}(l) + \mathbf{1}(k_i^*) v_i f_i(l, k_i^*)$$

$$l = k_0^*, \dots, k, \quad i = 1, \dots, N \quad (6b)$$

where  $\mathbf{1}(\cdot)$  is the unit step function. The hypothesis  $\mathcal{H}_0$  is interpreted as the absence of any recent abrupt changes in the random process  $z$ , and it assumes a specific realization  $a^{\mathcal{H}_0}$  for the process  $z$ , whereas the hypothesis  $\mathcal{H}_i$  corresponds to the occurrence of an abrupt change, of shape  $f_i$ , starting at time instant  $k_i^*$ . All of the hypotheses imply that only a single abrupt change can occur in the interval  $[k_0^*, k]$ . In this context, it is clear how the parameters  $k_i^*(k)$  should be chosen at each  $k$ : because the length of the time interval between successive abrupt changes has been assumed to be bounded from below by  $w^*$ , the parameters must be chosen so that  $(k - w^*) < k_i^*(k) < k$  for all  $i = 1, \dots, N$ . It is hence implied that all of the abrupt changes outside the maximal sliding window  $[k - w^*, k]$  have been detected and isolated prior to  $k$ .

In situations where  $w^*$  is large, it can be desirable to employ a sliding window smaller than the maximal sliding window to reduce the

computational load. The resulting effective sliding window (ESW) has a width  $w_{\text{eff}}^* < w^*$  and contains all of the hypotheses with an onset time in the interval  $(k - w_{\text{eff}}^*) < k_i^*(k) < k$ . The detector loses little by employing an ESW provided that  $w_{\text{eff}}^*$  is sufficiently large and that some additional hypotheses are sparsely distributed over the interval  $(k - w^*) < k_i^*(k) \leq (k - w_{\text{eff}}^*)$ , as discussed in Ref. 6. For the purpose of isolating the abrupt change, one of the hypotheses that previously slid out of the ESW can be included as a member of the set of additional hypotheses. This additional hypothesis keeps track of a detected change whenever it slides out of the ESW.

**B. Reference Kalman Filter**

To evaluate the likelihood of the individual hypotheses, a reference Kalman filter is implemented for the system (1) and (2), based on the assumption that hypothesis  $\mathcal{H}_0$  is true:

$$\hat{x}(k+1|k) = F(k)\hat{x}(k|k) + G_1(k)u(k) + G_2(k)a^{\mathcal{H}_0}(k) \quad (7)$$

$$\hat{x}(k|k) = \hat{x}(k|k-1) + K(k)\gamma(k) \quad (8)$$

where  $a^{\mathcal{H}_0}$  is the assumed realization for the process  $z$ . The measurement residual  $\gamma(k)$  is

$$\gamma(k) = y_m(k) - H(k)\hat{x}(k|k-1) \quad (9)$$

The gain  $K(k)$ , the state estimation covariance  $P(k|k)$ , and the residual covariance  $V(k)$  satisfy the Kalman-filter Riccati equation, solved recursively by

$$K(k) = P(k|k-1)H^T(k)V^{-1}(k) \quad (10)$$

$$P(k+1|k) = F(k)P(k|k)F^T(k) + Q_w(k) \quad (11)$$

$$P(k|k) = P(k|k-1) - K(k)H(k)P(k|k-1) \quad (12)$$

$$V(k) = H(k)P(k|k-1)H^T(k) + Q_\eta(k) \quad (13)$$

To calculate the likelihood ratios, the outputs needed from the reference Kalman filter are  $K(k)$ ,  $\gamma(k)$ , and  $V(k)$ .

**C. Normalized Signatures**

As mentioned earlier, the reference Kalman filter is matched to an hypothesis assuming a realization  $a^{\mathcal{H}_0}$  for the process  $z$ . Whenever an abrupt change occurs, the difference between the true realization of  $z$  and the one employed by the Kalman filter manifests itself by a drift in the mean of the residuals (see Ref. 1, pp. 238–240). This drift is the so-called signature of the abrupt change.

By assuming a normalized magnitude for the abrupt change, that is, by employing a signature shape  $f_i(k, k_i^*)$ , a normalized signature  $\rho(k, i)$  can be defined. The latter is recursively calculated as the product<sup>9</sup>

$$\rho(k, i) = H(k)\Gamma(k, i), \quad i \in \{1, \dots, N\} \quad (14)$$

where

$$\Gamma(l, i) = G_2(k)f_i(l, k_i^*) + \mathcal{F}(l-1)\Gamma(l-1, i)$$

$$l = k_i^* + 1, \dots, k \quad (15a)$$

$$\Gamma(k_i^*, i) = 0 \quad (15b)$$

and

$$\mathcal{F}(l-1) \triangleq F(k)[I - K(l-1)H(k)]$$

$$l = k_i^* + 1, \dots, k \quad (15c)$$

The signature of an abrupt change and the normalized signature are related by a scaling factor. The value of this scaling factor is calculated as the ratio between the abrupt change and the shape of this abrupt change, that is, the scaling factor is the change intensity  $v_i$  defined earlier.

*Remark 1:* For the purpose of change detection, the signature of a change should be large. Hence, the reference Kalman filter should be characterized by a low bandwidth, as then the signature will be more pronounced after a change occurs.

#### D. Log-Likelihood Ratios

To calculate the log-likelihood ratios, it is required to specify the realization of the process  $z$  after the abrupt change. Because the latter is unknown, its ML estimate is used instead. The ML estimate of the process  $z$  is obtained under the assumption that hypothesis  $\mathcal{H}_i$  is true. The generalized log-likelihood ratio  $l(k, i)$  corresponding to hypotheses  $\mathcal{H}_i$  and  $\mathcal{H}_0$  is then given by

$$l(k, i) = \frac{1}{2} [d^2(k, i)/J(k, i)], \quad i \in \{1, \dots, N\} \quad (16)$$

where  $J(k, i)$  is the Kullback–Leibler divergence<sup>9</sup> and  $d(k, i)$  is the signature correlation of hypothesis  $\mathcal{H}_i \in \mathcal{S}^k$ . The Kullback–Leibler divergence is a measure of the “distance” between the hypotheses  $\mathcal{H}_i$  and  $\mathcal{H}_0$  in  $\mathcal{S}^k$  and is calculated recursively as follows:

$$J(l, i) = J(l-1, i) + \rho^T(l, i)V^{-1}(l)\rho(k, i) \quad (17a)$$

$$l = k_i^* + 1, \dots, k$$

$$J(k_i^*, i) = 0 \quad (17b)$$

The signature correlation is interpreted as a least-squares estimate of the value of the abrupt change, assuming that  $\mathcal{H}_i$  is true and that no prior information about the value of the abrupt change is available.<sup>9</sup> It is recursively calculated as follows:

$$d(l, i) = d(l-1, i) + \rho^T(l, i)V^{-1}(l)\gamma(l) \quad (18a)$$

$$l = k_i^* + 1, \dots, k$$

$$d(k_i^*, i) = 0 \quad (18b)$$

#### E. GLR Test

The GLR test establishes the validity of the hypotheses. The test is performed in two stages. First, the index  $i_k^*$  of the hypothesis maximizing the log-likelihood ratios is determined:

$$i_k^* = \arg \max_{i \in \{1, \dots, N\}} \{l(k, i)\} \quad (19)$$

Next, the validity of the most likely hypothesis  $\mathcal{H}_{i_k^*}$  is assessed by comparing the maximized log-likelihood ratio with the value of a preselected threshold  $h$ :

$$l(k, i_k^*) \underset{\mathcal{H}_{i_k^*}}{\overset{\mathcal{H}_0}{\geq}} h \quad (20)$$

and the detection indicator  $\mathcal{E}(k)$  is set accordingly:

$$\mathcal{E}(k) = \begin{cases} 0 & \mathcal{H}_0 \text{ is true} \\ 1 & \mathcal{H}_{i_k^*} \text{ is true} \end{cases} \quad (21)$$

The value of  $h$  is selected as a function of the predefined probability of false alarm  $\alpha$ . It can be shown that this probability can be computed from a  $\chi^2$  distribution with one degree of freedom,<sup>9</sup> so that the value of  $h$  satisfies

$$\alpha = \int_h^\infty \chi^2(u) du \quad (22)$$

When an upper bound in the magnitude of the abrupt change is known a priori, the GLR test can incorporate this additional information by modifying Eq. (19) as follows (see Ref. 1, p. 53):

$$i_k^* = \arg \max_{i \in \{1, \dots, N\}} \{l(k, i) | \hat{z}(k, i) < z_{\text{ML}}^{\text{max}}\} \quad (23)$$

where  $\hat{z}(k, i)$  is the hypothesis-matched estimate of the abrupt change and  $z_{\text{ML}}^{\text{max}}$  is an upper bound on the magnitude of this estimate. The value of  $z_{\text{ML}}^{\text{max}}$  should be larger than the a priori known upper bound, to allow for the presence of estimation errors in  $\hat{z}(k, i)$ . The estimate  $\hat{z}(k, i)$  is given by

$$\hat{z}(k, i) \triangleq a^{\mathcal{H}_0}(k) + \hat{v}(k, i) f_i(k, k_i^*) \quad (24)$$

In Eq. (24), the scaling factor  $\hat{v}(k, i)$  matches the shape employed by hypothesis  $\mathcal{H}_i$  with the estimate of  $z$  and is calculated by

$$\hat{v}(k, i) = d(k, i)/J(k, i) \quad (25)$$

#### F. ML Estimates

The GLR detector provides the ML estimate  $\hat{k}^*$  of the onset time of the abrupt change and the ML estimate  $\hat{z}_{\text{ML}}$  of the value of the abrupt change. The ML estimate  $\hat{k}^*$  is given by

$$\hat{k}^*(k) = \begin{cases} \hat{k}_0^*(k) & \mathcal{E}(k) = 0 \\ \hat{k}_i^*(k) & \mathcal{E}(k) = 1 \end{cases} \quad (26)$$

where  $\hat{k}_0^*$  and  $\hat{k}_i^*$  are the time instants of the last confirmed abrupt change and of the hypothesis of index  $i_k^*$ , respectively.

$$\hat{k}_0^*(k) = \hat{k}_0^*(k-1), \quad \hat{k}_0^*(0) = 0 \quad (27)$$

The value of  $\hat{k}_0^*(k-1)$  is updated by the reinitialization module described in the next subsection. The ML estimate  $\hat{z}_{\text{ML}}$  is given by

$$\hat{z}_{\text{ML}}(k) = \begin{cases} a^{\mathcal{H}_0}(k) & \mathcal{E}(k) = 0 \\ a^{\mathcal{H}_0}(k) + \hat{v}(k, i_k^*) f_{i_k^*}(k, k_{i_k^*}^*) & \mathcal{E}(k) = 1 \end{cases} \quad (28)$$

#### G. Reinitialization Procedure

The purpose of the reinitialization of the detector is to allow for the detection of more than one abrupt change. The time instant of this reinitialization is application dependent. In fault detection applications, for which no accurate isolation of the change is required, the reinitialization is usually carried out immediately after the detection of an abrupt change. In target tracking applications, the reinitialization is delayed to allow for a more accurate isolation of the target maneuver characteristics. Hence, in this work a reinitialization of the standard GLR detector, indicated by  $\mathcal{E}^R(k) = 1$ , is performed whenever both an abrupt change is detected, and the ML estimate of the time instant of the change is located at the lower end of the maximal sliding window, that is,

$$\mathcal{E}^R(k) = \begin{cases} 1 & \{\mathcal{E}(k) = 1\} \wedge \{\hat{k}^* = k - w^*\} \\ 0 & \text{otherwise} \end{cases} \quad (29)$$

The reinitialization is carried out by modifying the hypothesis  $\mathcal{H}_0$  so that it encapsulates the history of the process  $z$  prior to the lower end of the effective sliding window and by discarding the previously collected measurements. Such a reinitialization can be performed as follows<sup>7,9</sup>:

1) The reference Kalman filter is matched to the hypothesis  $\mathcal{H}_{i_k^*}$  by setting

$$a_{\text{new}}^{\mathcal{H}_0}(l) = a_{\text{old}}^{\mathcal{H}_0}(l) + \hat{v}(k, i_k^*) f_{i_k^*}(l, k_{i_k^*}^*), \quad l = k, \dots \quad (30)$$

$$\hat{x}(k|k)_{\text{new}}^{\mathcal{H}_0} = \hat{x}(k|k)_{\text{old}}^{\mathcal{H}_0} + \hat{v}(k, i_k^*) \Upsilon(k, i_k^*) \quad (31)$$

$$P(k|k)_{\text{new}}^{\mathcal{H}_0} = P(k|k)_{\text{old}}^{\mathcal{H}_0} + \Upsilon(k, i_k^*) J^{-1}(k, i_k^*) \Upsilon^T(k, i_k^*) \quad (32)$$

where

$$\Upsilon(k, i_k^*) \triangleq [I - K(k)H(k)]\Gamma(k, i_k^*) \quad (33)$$

and the subscripts old and new denote variables before and after reinitialization, respectively, and the superscript  $\mathcal{H}_0$  denotes variables employed by the reference Kalman filter.

2) The likelihood ratios are reset to zero by discarding the already collected information:

$$\Gamma(k, i) = 0, \quad d(k, i) = 0, \quad J(k, i) = 0$$

$$i \in \{1, \dots, N\} \quad (34)$$

3) The information about the time instant of the confirmed abrupt change is preserved within  $\hat{k}_0^*$ :

$$\hat{k}_0^*(k) = k^*(k) \quad (35)$$

#### IV. Adaptive- $\mathcal{H}_0$ GLR Detector

The standard GLR algorithm of the preceding section is based on the underlying assumption that the chosen realization  $a^{\mathcal{H}_0}$  is indeed the true realization of the process  $z$  before the onset of the abrupt change. In many realistic detection scenarios, this is, however, seldom the case. To remedy this situation, an improved and extended version of the standard GLR detector is developed herein by enabling the reference acceleration for hypothesis  $\mathcal{H}_0$  to be adapted online. The flowchart of the adaptive- $\mathcal{H}_0$  GLR detector is shown in Fig. 3. Compared to the standard GLR detector, the adaptive- $\mathcal{H}_0$  GLR detector has one more component termed “ $\mathcal{H}_0$ -adaptation.” Four other components of the standard GLR detector are also modified or augmented: the set of hypotheses  $\mathcal{S}_a^k$ , the GLR test, the ML estimates, and the reinitialization procedure. The calculations of the normalized signatures and of the log-likelihood ratios are similar to those of the standard GLR detector; however, in the new algorithm they employ the augmented set of hypotheses.

##### A. Augmented Set of Hypotheses

The original set of hypotheses [Eqs. (6)] is now augmented with hypotheses whose purpose is to describe admissible shapes for a mismatch between the true realization of the process  $z$  and the realization assumed for  $a^{\mathcal{H}_0}$ . These additional hypotheses are analogous to  $\mathcal{H}_0$  in the sense that they assume the absence of abrupt changes within the maximal sliding window. For simplicity in the exposition, only a single such additional hypothesis is considered here. Let  $(\cdot)_{N+1}$  designate quantities associated with this additional hypothesis  $\mathcal{H}_{N+1}$ , defined as

$$\mathcal{H}_{N+1}: z(l) = a^{\mathcal{H}_0}(l) + v_{N+1} f_{N+1}(l, k_0^*), \quad l = k_0^*, \dots, k \quad (36)$$

where  $f_{N+1}(\cdot, k_0^*)$  is the shape assumed for the mismatch and  $v_{N+1}$  is the intensity of the mismatch. The augmented set of hypotheses then becomes  $\mathcal{S}_a^k = \{\mathcal{H}_0, \mathcal{H}_1, \dots, \mathcal{H}_N, \mathcal{H}_{N+1}\}$ .

##### B. Modified GLR Test

The GLR test now has the double task of 1) establishing the validity of the hypotheses, as before and 2) distinguishing between the event of an abrupt change in the process  $z$  and the event of a mismatch in the realization  $a^{\mathcal{H}_0}$ . The task of establishing the validity of the hypotheses is carried out as in the standard GLR detector, but the index  $i^*$  is now determined according to

$$i_k^* = \arg \max_{i \in \{1, \dots, N, N+1\}} \left\{ \beta(i) l(k, i) \mid \|\hat{z}(k, i)\| < z_{\text{ML}}^{\text{max}} \right\} \quad (37)$$

where the factor  $\beta$  is selected such that  $\beta(i) = 1$  for  $i \in \{1, \dots, N\}$  and  $\beta(N+1) \geq 1$ . The purpose of the factor  $\beta$  is to enable the algorithm to favor the selection of the hypothesis  $\mathcal{H}_{N+1}$  whenever the available information is not sufficient for the task of distinguishing between the onset of an abrupt change and a mismatch in  $a^{\mathcal{H}_0}$ . The validity of the most likely hypothesis  $\mathcal{H}_{i^*}$  is assessed by comparing the maximized log-likelihood ratio with the value of a preselected threshold  $h$ :

$$l(k, i_k^*) \underset{\mathcal{H}_{i_k^*}}{\overset{\mathcal{H}_0}{\geq}} h \quad (38)$$

and the value of the detection indicator  $\mathcal{E}(k)$  is set by Eq. (21), similarly to the standard GLR detector.

The additional task, of deciding about the type of the event, is carried out by introducing a complementary binary variable  $\mathcal{E}^0$  whose value is set according to the rule:

$$\mathcal{E}^0(k) = \begin{cases} 0 & \{\mathcal{H}_{i_k^*} \text{ is true}\} \wedge \{i_k^* \neq N+1\} \\ 1 & \{\mathcal{H}_{i_k^*} \text{ is true}\} \wedge \{i_k^* = N+1\} \end{cases} \quad (39)$$

In Eq. (39),  $\mathcal{E}^0(k) = 0$  indicates the event of an abrupt change in the process  $z$ , whereas  $\mathcal{E}^0(k) = 1$  indicates the event of a mismatch in the reference realization  $a^{\mathcal{H}_0}$ .

##### C. Modified ML Estimates

The interpretation of the ML estimates provided by the detector depends on the type of event detected in the earlier stage. In the event of an abrupt change [ $\mathcal{E}^0(k) = 0$ ], there are two ML estimates, and they concern the onset time instant and the realization of the abrupt change. These two ML estimates are calculated as in the standard GLR detector using Eqs. (26) and (28), respectively. In the event of a mismatch [ $\mathcal{E}^0(k) = 1$ ], there is only one ML estimate, which is the value of the mismatch. There is no estimate of the onset time of the mismatch in this case because the onset time instant of the realization  $a^{\mathcal{H}_0}$  is already known. The ML estimate  $\hat{a}^{\mathcal{H}_0}$  of the

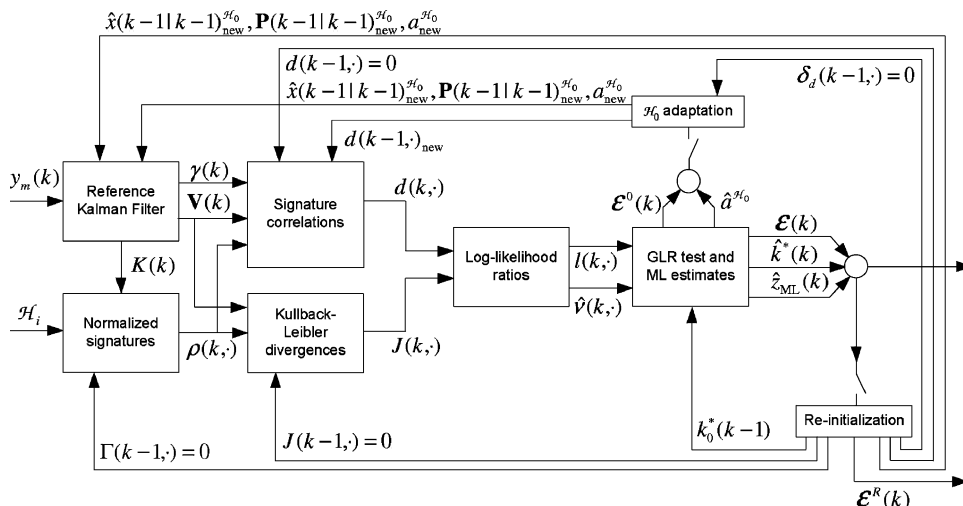


Fig. 3 Schematic flow diagram of the adaptive- $\mathcal{H}_0$  GLR detector.

reference realization is given by

$$\hat{a}^{\mathcal{H}_0}(l) = a^{\mathcal{H}_0}(l) + \hat{v}(k, N+1)f_{N+1}(l, k_0^*) \quad l = k_0^*, \dots \quad (40)$$

#### D. Adaptation of Hypothesis $\mathcal{H}_0$

An adaptation of hypothesis  $\mathcal{H}_0$  is performed whenever an error in the reference realization employed by the hypothesis  $\mathcal{H}_0$  is detected, that is, whenever  $\mathcal{E}^0(k) = 1$ . For consistency with the newly adapted reference realization, the likelihood ratios, which were calculated with respect to the erroneous reference realization, must be corrected.

*Proposition 1:* The adaptation of the  $\mathcal{H}_0$  hypothesis involves introducing the following corrections to the reference Kalman filter and the signature correlations:

$$a_{\text{new}}^{\mathcal{H}_0} = \hat{a}^{\mathcal{H}_0} \quad (41)$$

$$\hat{x}(k|k)_{\text{new}}^{\mathcal{H}_0} = \hat{x}(k|k)_{\text{old}}^{\mathcal{H}_0} + \hat{v}(k, N+1)\Upsilon(k, N+1) \quad (42)$$

$$P(k|k)_{\text{new}}^{\mathcal{H}_0} = P(k|k)_{\text{old}}^{\mathcal{H}_0} + \Upsilon(k, N+1)J^{-1}(k, N+1)\Upsilon^T(k, N+1) \quad (43)$$

$$d(k, i)_{\text{new}} = d(k, i)_{\text{old}} - \hat{v}(k, N+1)\delta_d(k, i) \quad i \in \{1, \dots, N, N+1\} \quad (44)$$

where the subscripts old and new denote variables before and after adaptation and where  $\delta_d(k, i)$  is obtained from the recursion:

$$\delta_d(l, i) = \delta_d(l-1, i) + \rho^T(l, i)V^{-1}(l)\rho(l, N+1) \quad l = k_i^* + 1, \dots, k \quad (45a)$$

$$\delta_d(k_i^*, i) = 0 \quad (45b)$$

*Proof:* Equation (41) corrects the realization  $a^{\mathcal{H}_0}$ , employed by the reference Kalman filter, by adopting the ML estimate of the realization of the process  $z$ . This modification of  $a^{\mathcal{H}_0}$  requires a corresponding correction of the state estimate and the associated estimation error covariance (previously calculated by the reference Kalman filter). These corrections are provided by Eqs. (42) and (43) (Ref. 12), respectively. The adaptation of the  $a^{\mathcal{H}_0}$  realization does not require the correction of the normalized signatures and the Kullback–Leibler divergences because they are not functions of  $a^{\mathcal{H}_0}$ . However, the signature correlations are functions of  $a^{\mathcal{H}_0}$ , and so they need to be corrected. The signature correlation correction, stated in Eq. (44), is proven next.

Let  $a_{\text{new}}^{\mathcal{H}_0}$  be the reference realization, adapted using hypothesis  $\mathcal{H}_{N+1}$ , and let  $a_{\text{old}}^{\mathcal{H}_0}$  be the reference realization before the adaptation. Let  $d(k, i)_{\text{old}}$  be the signature correlation calculated using  $a_{\text{old}}^{\mathcal{H}_0}$ , and let  $d(k, i)_{\text{new}}$  be the signature correlation calculated using  $a_{\text{new}}^{\mathcal{H}_0}$ . These signature correlations are, according to Eq. (18a),

$$d(k, i)_{\text{new}} = d(k-1, i)_{\text{new}} + \rho^T(k, i)V^{-1}(k)\gamma_{\text{new}}(k) \quad (46)$$

$$d(k, i)_{\text{old}} = d(k-1, i)_{\text{old}} + \rho^T(k, i)V^{-1}(k)\gamma_{\text{old}}(k) \quad (47)$$

where  $\gamma_{\text{new}}$  and  $\gamma_{\text{old}}$  are the residuals of reference Kalman filters employing  $a_{\text{new}}^{\mathcal{H}_0}$  or  $a_{\text{old}}^{\mathcal{H}_0}$ , respectively. The distributions of the residuals  $\gamma_{\text{new}}$  and  $\gamma_{\text{old}}$  are

$$\gamma(k)_{\text{new}} \sim \mathcal{N}[b(k), V(k)] \quad (48)$$

$$\gamma(k)_{\text{old}} \sim \mathcal{N}[b(k) + \hat{v}(k, N+1)_{\text{old}}\rho(k, N+1), V(k)] \quad (49)$$

where  $b$  is some bias,  $\rho(k, N+1)$  is the normalized signature of hypothesis  $\mathcal{H}_{N+1}$  [see Eq. (14)], and  $\hat{v}(k, N+1)_{\text{old}}$  is the scaling factor associated with  $\mathcal{H}_{N+1}$  when  $a_{\text{old}}^{\mathcal{H}_0}$  is employed [see Eq. (25)]. Whenever the realization  $a_{\text{new}}^{\mathcal{H}_0}$  matches the true realization of the process  $z$ , the bias  $b$  is identically zero (see Ref. 1, p. 240). Whenever the realization  $a_{\text{new}}^{\mathcal{H}_0}$  does not match the true realization of the process

$z$ , the bias  $b$  is nonzero, and, by virtue of linearity, it is the same in both Eqs. (48) and (49). Hence, using Eqs. (48) and (49) in Eqs. (46) and (47), the following key relation is obtained:

$$d(k, i)_{\text{new}} - d(k, i)_{\text{old}} = d(k-1, i)_{\text{new}} - d(k-1, i)_{\text{old}} - \hat{v}(k, N+1)_{\text{old}}\rho^T(k, i)V^{-1}(k)\rho(k, N+1) \quad (50)$$

From the preceding relation and by observing that  $d(k_i^*, i)_{\text{new}} = d(k_i^*, i)_{\text{old}} = 0$ , it follows that the relation between the signature correlations can be rewritten as

$$d(k, i)_{\text{new}} = d(k, i)_{\text{old}} - \hat{v}(k, N+1)_{\text{old}}\delta_d(k, i) \quad (51)$$

where

$$\delta_d(k, i) \triangleq \sum_{j=k_i^*}^k \rho^T(j, i)V^{-1}(j)\rho(j, N+1) \quad (52)$$

The normalized correction term  $\delta_d(k, i)$  can be interpreted as a correlation between the normalized signatures of the hypotheses  $\mathcal{H}_i$  and  $\mathcal{H}_{N+1}$ . Rewriting Eq. (52) in a recursive form finally yields Eqs. (45).  $\square$

Finally, the reinitialization procedure is carried out similarly to the reinitialization in the standard GLR detector, with the addition that the  $\mathcal{H}_0$  adaptation module must also be reinitialized, whenever  $\mathcal{E}^R(k) = 1$ , by setting

$$\delta_d(k, i) = 0, \quad i \in \{1, \dots, N, N+1\} \quad (53)$$

## V. Application to Pursuit-Evasion Endgame

The effectiveness of the adaptive- $\mathcal{H}_0$  GLR detector is demonstrated via an application to a pursuit-evasion endgame between an interceptor missile (the pursuer) and a maneuvering TBM (the evader). Only the detection and identification performance of the new algorithm is examined; the resulting performance of the entire homing loop (incorporating the new detector) in a similar example is examined in a companion paper.<sup>13</sup>

The strategy of the evader consists of a bang-bang maneuver with a single switch over the time interval of the engagement. The linearized system is represented by Eqs. (1) and (2). The known input  $u$  is the acceleration command of the pursuer, and the unknown input subject to additive abrupt changes  $z$  is interpreted as the evader's acceleration command. The engagement's mathematical model is described next, where the notation  $(\ )_E$  and  $(\ )_P$  is used to denote evader- and pursuer-related variables, respectively.

### A. Endgame Mathematical Model

The interception endgame is a short-horizon terminal control problem describing the pursuit of a maneuverable target by a guided missile. The information structure in such a scenario is generally imperfect. It is characterized by noise-corrupted measurements, acquired by the guided missile (pursuer), of the relative position of the target (evader). The evader has no information on the pursuer, but, being aware that an interception can occur, it can perform evasive maneuvers. Optimal control and differential game formulations of the problem,<sup>14,15</sup> as well as extensive simulation studies (see Ref. 16, p. 104), indicate that the most effective evasion maneuver is a judiciously timed direction reversal of the maximum maneuver. Because of its lack of information about the state of the pursuer, the evader cannot accurately time the required direction reversal. Because no maneuvering, or maneuvering in a fixed direction, might lead to a certain interception, the evasive strategy of the evader has to be random.

The stochastic dynamical model is expressed in the form:

$$\frac{dx}{dt} = f(x, a_P^c, a_E^c) \quad (54)$$

where  $x$  is the state of the system,  $a_P^c$  is the interceptor's control input, and  $a_E^c$  is the target's acceleration command. The three-dimensional nonlinear model (54) can be linearized about a nominal

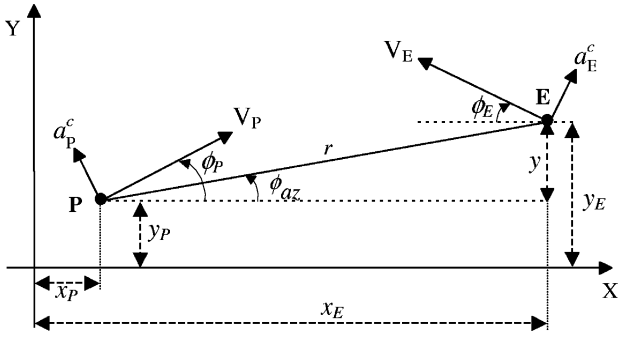


Fig. 4 Planar engagement geometry.

collision trajectory, determined by the initial line of sight and by the initial velocity vector of the evader. The pursuer heading angle  $\phi_{P_{col}}$  required for collision, is determined by

$$\sin(\phi_{P_{col}}) = (V_E/V_P) \sin[\phi_E(0)] \quad (55)$$

where  $V_P$  and  $V_E$  are the pursuer and evader velocities, respectively, and  $\phi_E$  is the heading angle of the evader. The linearization facilitates the decoupling of the three-dimensional model into two identical sets of planar equations in two perpendicular planes<sup>17</sup>; thus, a single model of linearized planar motion can be considered.

A schematic view of the planar endgame geometry is displayed in Fig. 4. An inertial coordinate system is used, whose  $X$  axis is aligned along the initial line of sight. Note that the respective velocity vectors are generally not aligned with the reference line of sight, but they remain close to the direction of the nominal collision course (55).

It is assumed that both the pursuer and the evader move with constant speeds and have bounded lateral accelerations  $|a_j^c| < (a_j^c)^{\max}$ ,  $j = \{E, P\}$ , that are perpendicular to the respective velocity vectors. Moreover, the maneuvering dynamics of both opponents can be approximated by first-order transfer functions with time constants  $\tau_P$  and  $\tau_E$ , respectively.

The (deterministic) nonlinear equations of the planar interception scenario are

$$\dot{x}_P = V_P \cos(\phi_P), \quad \dot{x}_E = V_E \cos(\phi_E) \quad (56a)$$

$$\dot{y}_P = V_P \sin(\phi_P), \quad \dot{y}_E = V_E \sin(\phi_E) \quad (56b)$$

$$\dot{\phi}_P = a_P/V_P, \quad \dot{\phi}_E = a_E/V_E \quad (56c)$$

$$\dot{a}_P = (a_P^c - a_P)/\tau_P, \quad \dot{a}_E = (a_E^c - a_E)/\tau_E \quad (56d)$$

where  $x_P$  and  $y_P$  are the positions of the pursuer along the  $X$  and  $Y$  axes, respectively;  $x_E$  and  $y_E$  are the positions of the evader along the  $X$  and  $Y$  axes, respectively; and  $a_P$  and  $a_E$  are the lateral accelerations of the pursuer and evader, respectively.

To facilitate linearization, it is assumed that the heading angles  $\phi_P$  and  $\phi_E$  are close to the directions of the nominal collision course (55). Let

$$x = [x_1 \quad x_2 \quad x_3 \quad x_4]^T \triangleq \left[ y \quad \frac{dy}{dt} \quad a_E \quad a_P \right]^T \quad (57)$$

be the state vector of the linearized problem, where  $y \triangleq y_E - y_P$  is the lateral separation between the evader and the pursuer, and  $dy/dt$  is the relative lateral velocity. The corresponding linearized differential equations of relative planar motion normal to the reference line and the respective initial conditions are

$$\dot{x}_1 = x_2, \quad x_1(0) = 0 \quad (58a)$$

$$\dot{x}_2 = x_3 - x_4, \quad x_2(0) = \left. \frac{dy}{dt} \right|_{t=0} \quad (58b)$$

$$\dot{x}_3 = \frac{a_E^c - x_3}{\tau_E}, \quad x_3(0) = 0 \quad (58c)$$

$$\dot{x}_4 = \frac{a_P^c - x_4}{\tau_P}, \quad x_4(0) = 0 \quad (58d)$$

The nonzero initial condition represents the difference between the respective initial velocity components that are not aligned with the initial (reference) line of sight. Because of the assumption of small deviations from the collision geometry, this difference is small compared with the components along the line of sight. The linearization also yields a constant closing velocity  $V_c$ :

$$V_c = V_P \cos(\phi_{P_{col}}) + V_E \cos[\phi_E(0)] \quad (59)$$

allowing the computation of the final time of the interception  $t_f$  for a given initial distance  $X_0$  as

$$t_f = X_0/V_c \quad (60)$$

Based on Eqs. (58), the matrices  $A$ ,  $B_1$ , and  $B_2$  of the continuous time-invariant system are

$$A = \begin{bmatrix} 0 & 1 & 0 & 0 \\ 0 & 0 & 1 & -1 \\ 0 & 0 & -1/\tau_E & 0 \\ 0 & 0 & 0 & -1/\tau_P \end{bmatrix}, \quad B_1 = \begin{bmatrix} 0 \\ 0 \\ 0 \\ 1/\tau_P \end{bmatrix}$$

$$B_2 = \begin{bmatrix} 0 \\ 0 \\ 1/\tau_E \\ 0 \end{bmatrix} \quad (61)$$

Thus, the matrices  $F$ ,  $G_1$ , and  $G_2$  of the discrete-time representation of the linear system over a sampling time interval  $\Delta$  are (see Ref. 18, p. 192)

$$F = \Phi(\Delta) = \mathcal{L}^{-1}(sI - A)^{-1}|_{\Delta}$$

$$= \begin{bmatrix} 1 & \Delta & \tau_E(\Delta - \Psi_E) & -\tau_P(\Delta - \Psi_P) \\ 0 & 1 & \Psi_E & -\Psi_P \\ 0 & 0 & e^{-\Delta/\tau_E} & 0 \\ 0 & 0 & 0 & e^{-\Delta/\tau_P} \end{bmatrix} \quad (62)$$

$$G_1 = \int_0^{\Delta} \Phi(\tau) B_1 d\tau = \begin{bmatrix} \tau_P(\Delta - \Psi_P) - \Delta^2/2 \\ \Psi_P - \Delta \\ 0 \\ 1 - e^{-\Delta/\tau_P} \end{bmatrix} \quad (63)$$

$$G_2 = \int_0^{\Delta} \Phi(\tau) B_2 d\tau = \begin{bmatrix} -\tau_E(\Delta - \Psi_E) + \Delta^2/2 \\ -\Psi_E + \Delta \\ 1 - e^{-\Delta/\tau_E} \\ 0 \end{bmatrix} \quad (64)$$

where

$$\Psi_i \triangleq \tau_i(1 - e^{-\Delta/\tau_i}), \quad i = \{P, E\} \quad (65)$$

Using an onboard sensor, the two measurements available to the pursuer are the relative angular displacement  $\phi_{az}$  of the evader with respect to an inertially fixed reference (e.g., the initial line of sight) and the range  $r$ . In the model, the range is measured perfectly, but the measurement of the relative angular position is corrupted by an additive noise  $\mu$  with a normal distribution. Using the small-angle approximation, the linearized measurement of the lateral separation  $y_m$  is

$$y_m(t) = r(t) \sin[\phi_{az}(t) + \mu(t)]$$

$$\approx r(t) \phi_{az}(t) + r(t) \mu(t)$$

$$\approx y(t) + r(t) \mu(t) \quad \mu(t) \sim \mathcal{N}(0, \sigma^2) \quad (66)$$

**Table 1** Simulation parameters

Parameter	Value
Pursuer velocity	$V_P = 2300$ m/s
Evader velocity	$V_E = 2700$ m/s
Pursuer maximal acceleration	$u^{\max} = 30$ g
Evader maximal acceleration	$z^{\max} = 15$ g
Pursuer dynamics time constant	$\tau_P = 0.2$ s
Evader dynamics time constant	$\tau_E = 0.2$ s
Initial distance	$X_0 = 20\,000$ m
Measurement rate	$f = 100$ Hz
False alarm probability	$\alpha = 0.001$
Measurement angular noise standard deviation	$\sigma = 0.1$ mrad
Maximal magnitude of $\hat{z}_{ML}$	$z_{ML}^{\max} = 100$ g

where  $r(t)$  denotes the slant range to the evader (assumed to be measured perfectly by the pursuer) and  $\mu$  is the angular measurement noise. Thus, the measurement matrix  $H$  and the measurement noise  $\eta$  in Eq. (2) are given by

$$H = [1 \ 0 \ 0 \ 0], \quad \eta(t) \triangleq r(t)\mu \sim \mathcal{N}(0, [r(t)\sigma]^2) \quad (67)$$

### B. Simulation Description

The simulation parameters are provided in Table 1. The measurement rate  $f$  determines the sampling time interval:  $\Delta = 1/f$ . The initial heading angles are zero, that is,  $\phi_P(0) = 0$  and  $\phi_E(0) = 0$ , and the initial evader's acceleration command is  $z(0) = 15$  g.

The parameters of the GLR detectors are the following. All of the hypotheses employ the same normalized shape for the evader's maneuver, and this common shape is a constant, that is,  $f_i(\cdot, \cdot) = 1$  for all  $i$ . The hypotheses differ only by the onset time instant for the maneuver. The standard GLR detector employs a maximal sliding window with a width  $w^* = 70$ , whereas the adaptive- $\mathcal{H}_0$  GLR detector employs a maximal sliding window of width  $w^* = 400$  and an effective sliding window of width  $w_{\text{eff}}^* = 70$ . For both detectors, the number of hypotheses in the sliding window is set to  $N = 70$ . The standard GLR detector requires a smaller maximal sliding window in order to have the ability of distinguishing between two events during the engagement: one event triggered by a possible mismatch between the realizations  $a^{\mathcal{H}_0}$  and  $z$ , and another event triggered by the evader's maneuver. In the case of the adaptive- $\mathcal{H}_0$  GLR detector, the detection of a mismatch does not prevent the detection of the evader's maneuver. As such, the adaptive- $\mathcal{H}_0$  GLR detector employs a larger maximal sliding window to improve the diagnosis of the evader's maneuver. To describe a possible mismatch between the realizations  $a^{\mathcal{H}_0}$  and  $z$ , the adaptive- $\mathcal{H}_0$  GLR detector employs a single hypothesis whose shape is a constant:  $f_{N+1}(\cdot, \cdot) = 1$ . The initial reference realization employed by the reference Kalman filter is  $a^{\mathcal{H}_0}(\cdot) = 0$ , that is,  $a^{\mathcal{H}_0}$  is initially mismatched with respect to  $z$ . The reference Kalman filter uses a nonzero process noise covariance matrix  $Q_k$  to provide some bandwidth to compensate for the uncertainties in the isolation of the abrupt change and for possible nonlinearities. This discrete-time process noise covariance matrix is computed as

$$Q_k = \int_0^\Delta \Phi(\tau) Q \Phi^T(\tau) d\tau, \quad Q = \text{diag}\{q_{11}, q_{22}, q_{33}, 0\} \quad (68)$$

where the transition matrix  $\Phi$  is provided in Eq. (62) and where  $q_{11} = 1$  m<sup>2</sup>,  $q_{22} = 10$  m<sup>2</sup>/s<sup>2</sup>, and  $q_{33} = 1$  m<sup>2</sup>/s<sup>4</sup>. The theoretical false alarm probability  $\alpha$  is used to select the threshold used for the abrupt change hypotheses in the GLR test, which is computed using Eq. (22) to be  $h = 10.83$ . Using a tuning process, the factor  $\beta(N+1)$ , employed by the GLR test in the adaptive- $\mathcal{H}_0$  GLR algorithm, is set to  $\beta(N+1) = 1.05$ . The value of the bound  $z_{ML}^{\max}$ , much larger than  $z^{\max}$ , is a soft constraint chosen so as to discard only the few hypotheses with an estimate of  $z$  obviously wrong, even when taking into account the worst possible estimation errors.

The detection statistics of the adaptive- $\mathcal{H}_0$  GLR detector are compared to those of the standard GLR detector. These statistics are

obtained by performing 40 Monte Carlo simulation studies employing each of the detectors. Each Monte Carlo simulation study is characterized by a different value for the onset time of the evader's maneuver. For each Monte Carlo simulation study, the engagement is repeated 1000 times; every repetition employs a different noise realization. The following criteria were chosen for the comparison: the observed false alarm probability, the observed missed detection probability, the average detection delay, the average error in the estimation of  $z$  during the maneuver, and the standard deviation of this estimation error.

To present the results, it is useful to define the time to go  $t_{go}$  and the time to go at the onset of the evader's maneuver  $tgo_{sw}$ :

$$t_{go} \triangleq t_f - t, \quad t \triangleq k\Delta \quad (69)$$

$$tgo_{sw} \triangleq t_f - t^*, \quad t^* \triangleq k^*\Delta \quad (70)$$

### C. Detection Statistics

A decision test (such as the GLR test) involves risks of making two types of false decisions: rejecting the null hypothesis when it is, in fact, true (type I error), and accepting the null hypothesis when it is, in fact, false (type II error) (see Ref. 19, p. 65). Here, the observed false alarm probability is calculated by dividing the ensemble average of false alarms before the onset of the evader's maneuver by the number of time instants before the onset. The observed false alarm probability (type I error) is shown in Fig. 5. As seen from Fig. 5, the adaptive- $\mathcal{H}_0$  GLR detector delivers a false alarm probability about four times smaller than that obtained by the standard GLR detector. The peak in the false alarm probability, at  $tgo_{sw} \in [3.3, 3.8]$  s, is interpreted as follows. Whenever the evader performs its maneuver close to the beginning of the engagement, the standard GLR detector cannot separate the event caused by a mismatch in  $a^{\mathcal{H}_0}$  and the event caused by the evader's maneuver. Because both events are present within the sliding window of the detector and because the detector has no single hypothesis that accounts for both, a larger false alarm probability results.

In terms of the observed miss detection probability (type II error, not shown here for conciseness), the standard and the adaptive- $\mathcal{H}_0$  GLR detectors behave almost identically. Both detectors are able to detect all abrupt changes occurring in the interval  $tgo_{sw} \in [0.3, 3.9]$  s, but are unable to detect changes occurring near the beginning or the end of the engagement. Near the beginning of the engagement, there is no sufficient information to reliably distinguish between the event of a change and an error in the initial conditions, whereas at the end of the engagement there is not enough time left to collect sufficient information to deliver a decision.

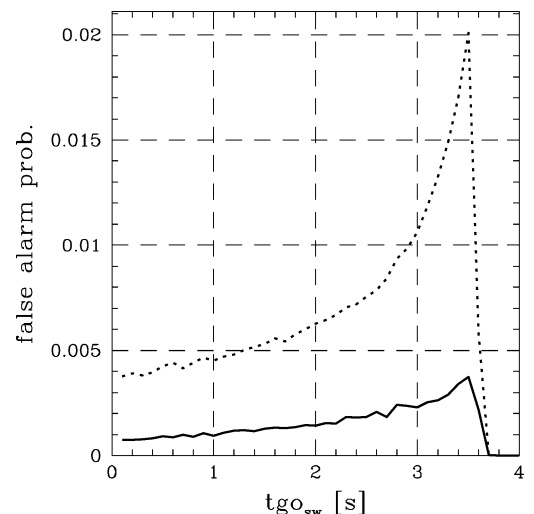


**Fig. 5** Probabilities of false alarm vs the time instant of the change: —, adaptive- $\mathcal{H}_0$  GLR detector; ···, standard GLR detector.

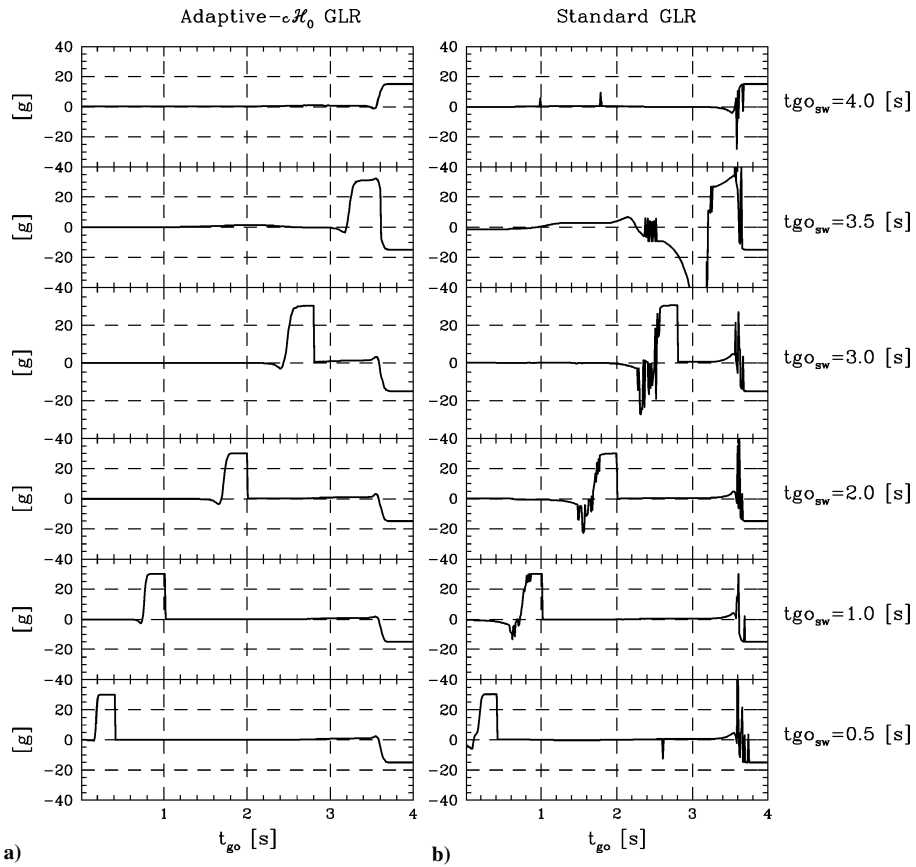


Fig. 6 Average error of the estimate of the evader's command acceleration for several onset time instant of the bang-bang maneuver: a) adaptive- $\mathcal{H}_0$  GLR detector and b) standard GLR detector.

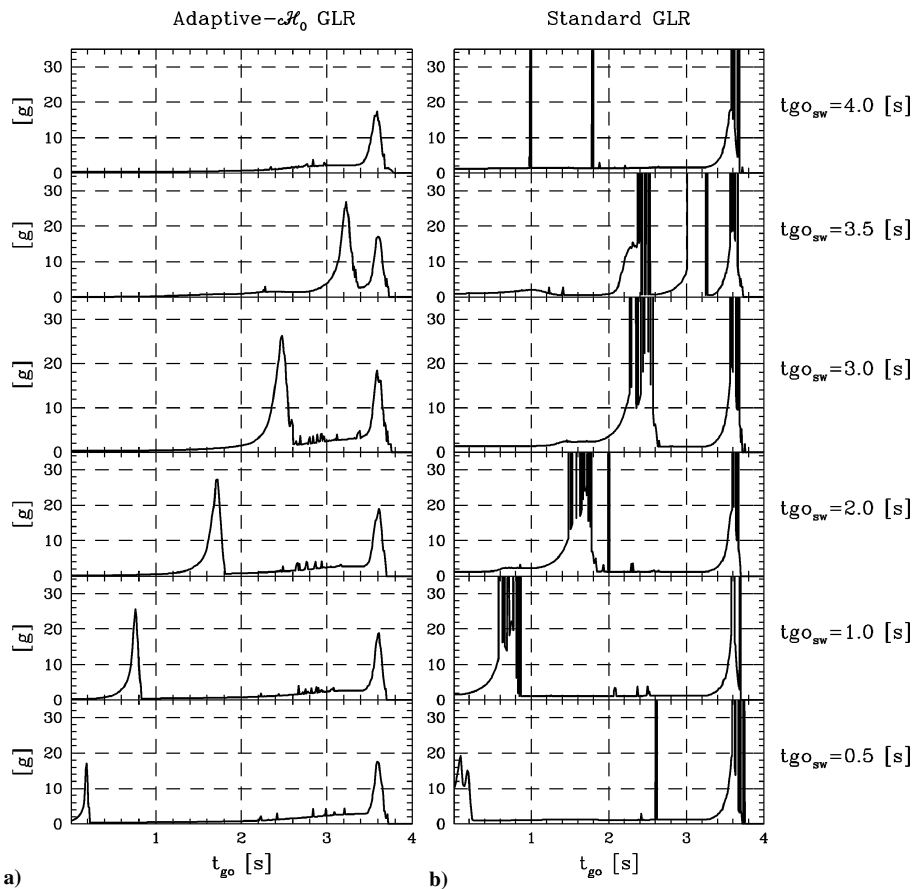


Fig. 7 Standard deviation of the estimation error of the evader's command acceleration for several onset time instant of the bang-bang maneuver: a) adaptive- $\mathcal{H}_0$  GLR detector and b) standard GLR detector.

Because of the necessity of collecting sufficient information to deliver a statistically significant decision, there is always a time delay between the onset time of the evader's maneuver and the time instant at which this maneuver is detected. The mean detection delay depends on the timing of the change ( $t_{go_{sw}}$ ). The observed value (not shown here for conciseness) is similar for both the adaptive- $\mathcal{H}_0$  and the standard GLR detectors and is an almost linear function of  $t_{go_{sw}}$ , monotonically increasing from 0.21 s (at  $t_{go_{sw}} = 0.3$  s) to 0.37 s (at  $t_{go_{sw}} = 3.6$  s). The longer detection time is because the angular noise is constant, and the displacement noise is proportional to the range.

The GLR detectors provide an estimate  $\hat{z}_{ML}$  of the true evader's acceleration command  $z$ . The mean and standard deviation of the estimation error,  $e(k) = \hat{z}_{ML}(k) - z(k)$ , are shown in Figs. 6 and 7, respectively. The results are presented for six different onset times of the evader's maneuver. In all cases, the initial mismatch in  $a^{H_0}$  is detected and first corrected at  $t_{go} \approx 3.6$  s. At that point, the average error in the estimate from the standard GLR detector demonstrates a much larger overshoot than the one from the adaptive- $\mathcal{H}_0$  GLR detector. Also, the pulse-like feature in the plots of Fig. 6 is generated by the evader's maneuver: the birth of the pulse happens at the onset of a maneuver, and its left slope corresponds to the actual detection of the maneuver. The width of the pulse is associated with the detection delay. Following the detection of the maneuver, both detectors exhibit an overshoot in the average error of the estimate. This overshoot is clearly much larger using the standard GLR detector and is particularly pronounced for  $t_{go_{sw}} = 3.5$  s. This is attributed to a mismatch in the employed  $a^{H_0}$  during the evader's maneuver. The adaptive- $\mathcal{H}_0$  GLR detector avoids this pitfall because of its ability to separate the event of a mismatch and the event of the onset of the evader's maneuver. Additionally, the standard GLR detector delivers many false alarms (manifested as spikes in the average error), compared to a negligible number of false alarms in the case of the adaptive- $\mathcal{H}_0$  GLR detector (no visible spikes in the average error).

The standard deviation of the estimation error  $\hat{z}_{ML}$  from the adaptive- $\mathcal{H}_0$  GLR detector is demonstrated to be much smaller than the one from the standard GLR detector (see Fig. 7). Moreover, the standard GLR detector fails to provide a consistent estimate of the evader's acceleration command; note the nonzero bias in the standard deviation plots in Fig. 7b. In contrast, the adaptive- $\mathcal{H}_0$  GLR detector can serve as a consistent filter.

## VI. Conclusions

A novel GLR-type detector that employs an adaptive formulation of one of its key ingredient hypotheses (the  $\mathcal{H}_0$  hypotheses) has been presented. The development of the new algorithm is motivated by the absence of sufficiently fast and reliable sequential detection schemes that are capable of detecting and identifying abrupt changes in unknown input processes, such as the acceleration commands of randomly maneuvering targets.

The novel adaptive- $\mathcal{H}_0$  GLR detector employs parametric families of input functions; the latter translate into parametric families of distributions for the observations. The distributions of the observations before and after the onset of a maneuver are estimated online as members of these families of distributions. Based on the estimated distributions, a decision concerning the occurrence (or absence) of a maneuver is made, and the characteristics of the maneuver are derived.

The new detector is implemented in the difficult case of tracking a randomly maneuvering tactical ballistic missile. Both the new scheme and the standard GLR detector are employed for the sake of comparing their performance. An extensive Monte Carlo simulation study is used to evaluate the main statistical properties of both detectors. The adaptive- $\mathcal{H}_0$  GLR detector is shown to outperform the standard GLR detector in that it achieves a lower observed false

alarm probability (about four times smaller than that achieved by the standard GLR), a more consistent detection delay, characterized by a smaller standard deviation, and a more consistent input estimate, characterized by a smaller average error and a smaller standard deviation. Also, in contradistinction with the standard GLR detector, the observed false alarm probability of the novel detector matches its theoretical prediction (the prespecified false alarm probability).

Based on the demonstrated superiority of the adaptive detector, it is concluded that the new scheme constitutes a powerful tool for the maneuver detection and identification of fast moving targets. The use of the adaptive detector in combination with advanced guidance laws in interception scenarios involving randomly maneuvering ballistic missiles is presented in a companion paper.

## References

- <sup>1</sup>Basseville, M., and Nikiforov, I., *Detection of Abrupt Changes—Theory and Applications*, Prentice-Hall, Englewood Cliffs, NJ, 1993.
- <sup>2</sup>Lai, T. L., "Sequential Change-point Detection in Quality Control and Dynamical Systems," *Journal of the Royal Statistical Society, Series B*, Vol. 57, No. 4, 1995, pp. 613–658.
- <sup>3</sup>Gustafsson, F., *Adaptive Filtering and Change Detection*, Wiley, New York, 2000, p. 218.
- <sup>4</sup>Shiryayev, A. N., "The Problem of the Most Rapid Detection of a Disturbance in a Stationary Process," *Soviet Mathematical Doklady*, Vol. 1, No. 2, 1961, pp. 795–799.
- <sup>5</sup>Vellekoop, M. L., "Rapid Detection, and Estimation of Abrupt Changes by Nonlinear Filtering," Ph.D. Dissertation, Imperial College of Science, Technology and Medicine, Dept. of Electrical and Electronic Engineering, London, Oct. 1997.
- <sup>6</sup>Lai, T. L., and Shan, Z., "Efficient Recursive Algorithms for Detection of Abrupt Changes in Signals and Systems," *IEEE Transactions on Automatic Control*, Vol. 44, No. 5, 1999, pp. 952–966.
- <sup>7</sup>Dowdle, J. R., Willisky, A. S., and Gully, S. W., "Nonlinear Generalized Likelihood Ratio Algorithms for Maneuver Detection and Estimation," *Proceedings of the American Control Conference*, IEEE Publications, Piscataway, NJ, 1982, pp. 985–987.
- <sup>8</sup>Korn, J., Gully, S. W., and Willisky, A. S., "Application of the Generalized Likelihood Ratio Algorithm to Maneuver Detection and Estimation," *Proceedings of the American Control Conference*, IEEE Publications, Piscataway, NJ, 1982, pp. 792–798.
- <sup>9</sup>Willisky, A. S., and Johns, H. L., "A Generalized Likelihood Ratio Approach to the Detection and Estimation of Jumps in Linear Systems," *IEEE Transactions on Automatic Control*, Vol. AC-21, No. 1, 1976, pp. 108–112.
- <sup>10</sup>McAulay, R. J., and Denlinger, E., "A Decision-Directed Adaptive Tracker," *IEEE Transactions on Aerospace and Electronic Systems*, Vol. 9, No. 2, 1973, pp. 229–236.
- <sup>11</sup>Dionne, D., Michalska, H., and Oshman, Y., "Terminal Missile Guidance Using a Semi-Markov Target Model," *Proceedings of the 16th IFAC Symposium on Automatic Control in Aerospace*, Vol. 2, Elsevier Science Ltd., Oxford, England, U.K., 2004, pp. 56–61.
- <sup>12</sup>Caglayan, A., and Lancraft, R., "Reinitialization Issues in Fault Tolerant Systems," *Proceedings of the American Control Conference*, IEEE Publications, Piscataway, NJ, 1983, pp. 952–955.
- <sup>13</sup>Dionne, D., Michalska, H., Shinar, J., and Oshman, Y., "Decision-Directed Adaptive Estimation and Guidance for an Interception Endgame," *Journal of Guidance, Control, and Dynamics* (submitted for publication).
- <sup>14</sup>Shinar, J., and Steinberg, D., "Analysis of Optimal Evasive Maneuvers Based on a Linearized Two-Dimensional Model," *Journal of Aircraft*, Vol. 14, Aug. 1977, pp. 795–802.
- <sup>15</sup>Shinar, J., and Glizer, V. Y., "Solution of a Delayed Information Linear Pursuit-Evasion Game with Bounded Controls," *International Game Theory Review*, Vol. 1, No. 3–4, 1999, pp. 197–217.
- <sup>16</sup>Zarchan, P., *Tactical and Strategic Missile Guidance*, 4th ed., Progress in Astronautics and Aeronautics, Vol. 199, AIAA, Reston, VA, 2002, p. 104.
- <sup>17</sup>Adler, F. P., "Missile Guidance by Three-Dimensional Proportional Navigation," *Journal of Applied Physics*, Vol. 27, No. 3, 1956, pp. 500–507.
- <sup>18</sup>Bar-Shalom, Y., and Li, X.-R., *Estimation and Tracking: Principles, Techniques and Software*, Artech House, Inc., Boston, 1993, p. 192.
- <sup>19</sup>Kay, S., *Fundamental of Statistical Signal Processing, Vol. 2: Detection Theory*, Prentice-Hall, Upper Saddle River, NJ, 1998, p. 65.